XIX International Conference on Water Resources
CMWR 2012
University of Illinois at Urbana-Champaign
June 17-22,2012

NUMERICAL MODELING OF OGEE CREST SPILLWAY AND TAINTER GATE STRUCTURE OF A DIVERSION DAM ON CAÑAR RIVER, ECUADOR

Viviana Morales∗, Talia E. Tokyay∗ and Marcelo Garcia∗

∗University of Illinois at Urbana-Champaign
Department of Civil and Environmental Engineering
205 N. Mathews, Urbana, IL 61801 USA
e-mail: morale25@illinois.edu

Key words: CFD models, Simulation, Spillway, Gate

Summary. The Guayas watershed sustains several economical activities such as agriculture and industrial shrimp aquaculture. Due to this activities this watershed has become an an important economical region of Ecuador. However, problems related with flooding, sediment transport and inefficient natural drainage badly affect the production capacity of the watershed. In order to overcome these problems, a series of hydraulic projects are planned to be built in the southeast of the Guayas watershed including three sub basins, the Bulubulu River, the Cañar River and the Naranjal River with a total extension of around $5,000\ km^2$. This study focuses on one of these projects, a diversion dam located on the Cañar River. This hydraulic structure is designed to divert part of the streamflow from its natural course to an artificial channel to improve the flood control in downstream region.

In this study, interaction of flow with these structures is analyzed using a three-dimensional finite volume code that uses transient volume of fluid (VOF) method to capture free surface profile.

1 INTRODUCTION

Diversion dams are hydraulic structures that are designed to divert all or a portion of the river flow from its natural course. The diversion dam under study was designed to control floods and stabilize the river course. The designed structure consists of a series of tainter gates that control the flow to the river side by side with a series of ogee crested spillways that divert the excess flow to a bypass channel.

Historically, the flow through hydraulic structures was analyzed and assessed through physical models. However, in the past three decades with the advent of high-performance computers, the study of fluid flow problems by means of Computational Fluid Dynamics (CFD) became possible. As a consequence, CFD grew into a cost-effective alternative that complements experimental and theoretical fluid dynamics.

In recent studies, combination of physical and numerical approaches were used to investigate flow over hydraulic structures. Some of these studies compare flow parameters over a standard ogee-crested spillway [1,2]. In [1,2], they utilized the commercial CFD package Flow-3D with the transient volume of fluid method (VOF) to capture free surface profile. Another recent study focused on numerical and experimental modeling of a bottom outlet[3]. The numerical simulation was developed in Fluent by using the VOF method and the k-ϵ turbulence model. In all these studies, reasonably good agreement, between the physical and numerical models were found.

In this study numerical simulations are being implemented primarily for the purpose of evaluating the design of the structures. Thus, a parametric study is conducted with the objective of investigating the flow field and the complex free surface profile over the ogee-crest spillway and under the gate of the diversion dam.

2 PHYSICAL MODELS

Physical modeling was conducted on two components of the diversion dam: ogee crest spillway with its stilling basin and gate structure with its dissipation basin. The physical models were designed per unit width by applying Reynolds and Froude numbers as similarity criteria to scale the hydraulic structures. The experiments were performed in the hydraulics laboratory of the University of Cuenca in Ecuador. A variable slope ARM-FIELD flume approximately 12.5 m long, 0.3 m wide and 0.46 m deep was utilized. Based on the dimensions of the flume, longitudinal scales of 1/16 and 1/20 were used for the ogee-crested spillway and the tainter gate, respectively.

3 NUMERICAL MODELS

A non-hydrostatic finite-volume code, which solves three dimensional Navier-Stokes Equations, was used in the numerical simulations. This code has been widely used in several studies that involve CFD modeling of hydraulic structures such as spillways. The (VOF) method together with k-ϵ turbulence model was implemented to developed a numerical model to simulate free surface flow over an ogee-crested spillway[4,5]. Similarly, the probable maximum flow over a system of spillways was investigated[6]. In all these studies the numerical results were validated against experimental work.

In our simulations the turbulence closure was satisfied by k-ω model. This model is based on the Wilcox k-ω model[7]. The transport equations of the turbulent kinetic energy, k, and the specific dissipation rate, ω, in standard k-ω model are given in Eqn.1 and 2. This model is an empirical based model. The production terms that appear in the equations of both k and ω, are shown to improve the accuracy of the model for predicting free-shear flows.

$$\frac{\partial(\rho k)}{\partial t} + \frac{\partial}{\partial x_i}(\rho k u_i) = \frac{\partial}{\partial x_j}\left(\Gamma_k \frac{\partial k}{\partial x_j}\right) + G_k - Y_k \tag{1}$$

$$\frac{\partial(\rho\omega)}{\partial t} + \frac{\partial}{\partial x_i}(\rho\omega u_i) = \frac{\partial}{\partial x_j}\left(\Gamma_\omega \frac{\partial \omega}{\partial x_j}\right) + G_\omega - Y_\omega \tag{2}$$

$\omega = \frac{k}{\varepsilon}, G_k$ represents the generation of turbulent kinetic energy due to mean velocity gradients. G_ω is the generation of w. Γ terms are for the effective diffusivity of k and ω. Meanwhile, Y terms are for the dissipation of k and ω due to turbulence.

Volume of Fluid Method (VOF) is used to simulate free-surface flow. This method permits to model two or more immiscible fluids by solving a single set of momentum equations and tracking the volume fraction of each of the fluids throughout the domain [8]. Air and water are the fluids selected for VOF simulations as the interface between these fluids represents the freesurface of a flow. The interface estimation is done by a high resolution differencing scheme known as Compressive Interface Capturing Scheme for Arbitrary Meshes (CICSAM)[9]. All operators are discretized using second order upwind scheme. Gravitational affects are also taken into account in the simulation.

The computational grid of ogee-crest spillway and its stilling basin has around $210,000$ hexahedral elements. While the gate structure and its dissipation basin is compound by $158,000$ hexahedral elements. Computational grids for both domains are given in Figure 1. Spillway simulations were carried on until total simulation time $tf \sim 50s$ and gate simulations were carried on until $tf \sim 35s$. It is worth mentioning that the grid quality was critical to achieve accuracy in the interface capturing.

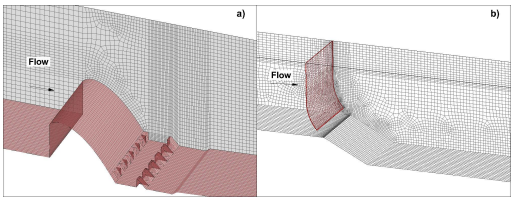

Figure 1: Computational grid used in numerical simulations; a) 3D view of the grid for the spillway and stilling basin;b)3D view of the grid for the gate and dissipation basin.

4 RESULTS

Six simulation scenarios were carried out using the operation conditions of the scaled physical model. Table 1 summarizes the input parameters from the simulations of flow over the spillway and under the gate, respectively. Figure 2 illustrates the relative location of measurement of these parameters along the simulation domains.

In Figure 3 isocontours of volume fraction fluid (VF) are shown for three simulation scenarios (S1, S2, S3) of the spillway and stilling basin. It is assumed that 0.35 <VF< 0.95 represents the interface between air and water in simulations. Below this interface in the figure, the VF 0.95, represents water. Figures 3a,b) illustrates a prototype flow of $1,345$ m^3/s corresponding to simulations S1 and S2. In Figure 3b) the dashed step, represents

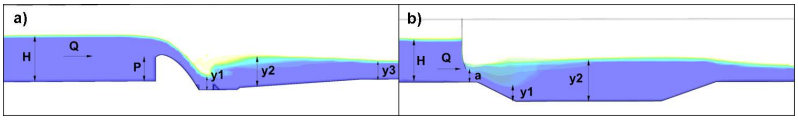

Figure 2: Sketch of flow profiles; a)Spillway; b)Gate.

	Model			**Prototype**				**Model**			**Prototype**		
	Q[1]	P [2]	y_3[3]	Q	P	y_3		Q[4]	H[5]	a[6]	Q	H	a
	[l/s]	[cm]	[cm]	[m^3/s]	[m]	[m]		[l/s]	[cm]	[cm]	[m^3/s]	[m]	[m]
S1	23.86	13.70	18.75	1345	2.19	3.00	G1	13.42	26.10	2.80	400	5.22	0.56
S2	23.86	6.55	18.75	1345	1.05	3.00	G2	13.42	28.80	3.10	400	5.76	0.62
S3	19	13.70	15.63	1100	2.19	2.50	G3	23.48	20.60	6.60	700	4.12	1.32

1 spillway volumetric flow rate, 2 height of the spillway crest with respect to channel bed, 3 downstream water depth, 4 gate volumetric flow rate, 5 gate's upstream water head, 6 gate opening

Table 1: Simulation parameters used in the physical and numerical models of the ogee crested spillway and tainter gate.

accumulation of sediment at the back of the spillway. In the experiments large size sediment is used to mimic such accumulation behind the spillway. However, in numerical simulations we simply used a step to reduce the height of the crest. Moreover, simulation S3 corresponds to a prototype flow of $1,100\ m^3/s$, which is the design flow of the structure. The free surface profile for this simulation is shown in Figure 3c). Finally, in Figure 3d) we are showing a picture of the experimental flow profile for the design flow conditions. It may be noted in all cases that the hydraulic jump is forced upstream and finally drowned, becoming a submerge jump[10]. The submersion condition, didn't permit us to observed the conjugated depths of the jump. Consequently, we assumed y_1 to be equal to height of the water nappe and y_2 was calculated with the Belangers Equation[11]. This analytical calculation prove the submersion of the jump.

4.1 Spillway Analysis

From Figure 3, the length and height of the submerged jump with respect to the spillway face and the basin was calculated. Based on all three simulations maximum length of the jump is estimated to be around 3.7m, while the height of the roller is estimated to be around 3.2m for design flow conditions. Moreover, good agreement between physical and numerical models is observe from Figures 3c,d). Comparison in terms of the length (l) and conjugate depth (y_2) of the jump is presented in Table 2. The percent difference ranges between 12%-21% for y_2 and between 3%-15% for l. Not considering the roughness effects in the numerical simulations might have caused this variation. Velocity distribution for the three simulations are illustrated in Figures 3e-g). In these figures the dash line represents the free surface which is defined by VF=0.6. The color band in these figures indicates velocity contours in the range from 0.10m/s to 1.2m/s. It may be noted that maximum

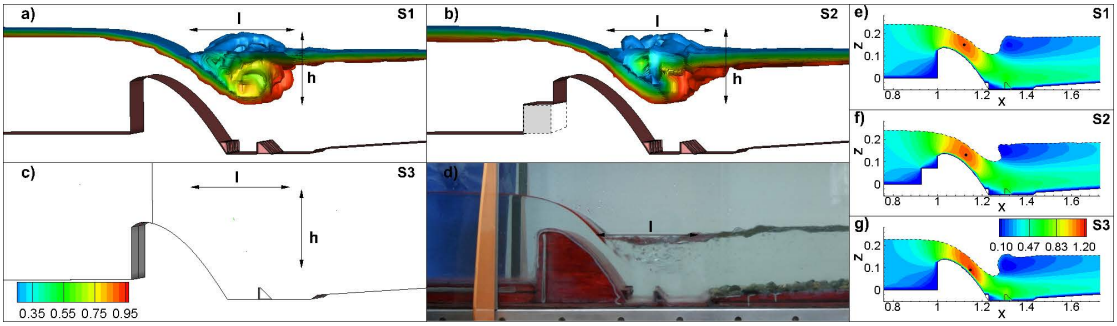

Figure 3: Free surface profile and velocity distribution throughout the simulation domain of the spillway; a)Free surface profile for simulation case S1; b)Free surface profile for simulation case S2; c)Free surface profile for simulation case S3; d) Picture of the physical model for equivalent conditions to S3 simulation; e)Velocity distribution for simulation case S1; f)Velocity distribution for simulation case S2; g)Velocity distribution for simulation case S3. Dot represents the location of maximum velocity.

	Physical		**Numerical**		**% Diff**			**Physical**		**Numerical**		**% Diff**	
	y_2 [1]	l [2]	y_2	l				v_{middle} [3]	v_{end} [4]	v_{middle}	v_{end}		
	[cm]	[cm]	[cm]	[cm]	[%]	[%]		[m/s]	[m/s]	[m/s]	[m/s]	[%]	[%]
S1	19.10	26.50	21.30	23.00	12	15	G1	0.23	0.20	0.35	0.25	54	28
S2	19.50	23.70	22.10	24.60	13	4	G2	0.32	0.19	0.30	0.24	5	23
S3	15.60	21.80	18.90	23.00	21	3	G3	0.36	0.31	0.38	0.35	6	11

1 hydraulic jump subcritical conjugate depth, 2 length of the hydraulic jump, 3 Velocity measured at the middle of the dissipation basin , 4 Velocity measured at the end of the dissipation basin

Table 2: Comparison between simulated and measured length and conjugate depth of the hydraulic jump formed in the spillway model and comparison between simulated and measured velocities at the middle and end of the dissipation basin of the gate.

velocities patches occurred over the middle section of the spillway face. As observed in Figure 3f), the high velocity patch travels further upstream as a consequence of having a smaller crest height. In Figure 3g) the patch of high velocities is elongated and enters further into the dissipation basin. We observed maximum velocities for the design flow case (S3). In prototype scale these velocities reach up to 4.65m/s. Due to resulting high velocities, erosion of the spillway face may occur for the given flow conditions. Moreover, we noted a large velocity reduction at the end of the basin. Thus, high energy dissipation takes place in the basin.

Additionally, we created two new simulations in order to observe the effect of the tail water depth in the free surface profile over the spillway and stilling basin. Unfortunately, experimentally these flow conditions were not investigated. We used simulation S1 as base scenario and lowered the tail water depth to create simulations S1", and S1'. Possible free surface profiles for the simulations are represented by the isosurfaces shown in Figures 4a-c). In these figures, we are showing resulting free surface profiles for tail water depths of 1.52m and 1.92m and 3m, respectively. For the first two cases, the hydraulic jump

sequent depth (y_2) is larger than the tail water depth (y_3). As a result, the jump recedes downstream and severe erosion would result in the basin[13].

Moreover, the effect of the tail water depth in the length (l), height (h) and location of the jump with respect to the spillway face (x_1) and the basin (y_1)is assessed from Figure 4d). We used the upstream water depth (H) to make the jump parameters and the tail water depth dimensionless. In Figure 4d) Y axis corresponds to the non-dimensional jump parameters and the X axis represents the dimensionless tail water depth. We observed a linear relation for x_1 and y_1, the smaller the tail water depth, the closer the jump gets to the face of the spillway and the bottom of the basin. However, when it comes to the length (l) and height (h) of the jump we were not able to see a linear relation. Therefore, we can not draw a clear conclusion for these parameters. However, it is clear that the perturbation travels further downstream of the dissipation basin, for the lowest tail water condition.

Furthermore, in Figures 4e-g) we present the influence of the tail water depth in the velocity distribution. In these figures the dash line represents the free surface which is defined by a value of VF= 0.6. We observed the higher velocities to occur for the lowest tail water depth case (S1"). Based on the simulation results, the maximum expected prototype velocity is 6.1m/s. Additionally, the velocity patch over the face of the spillway enters further into the basin for this case.

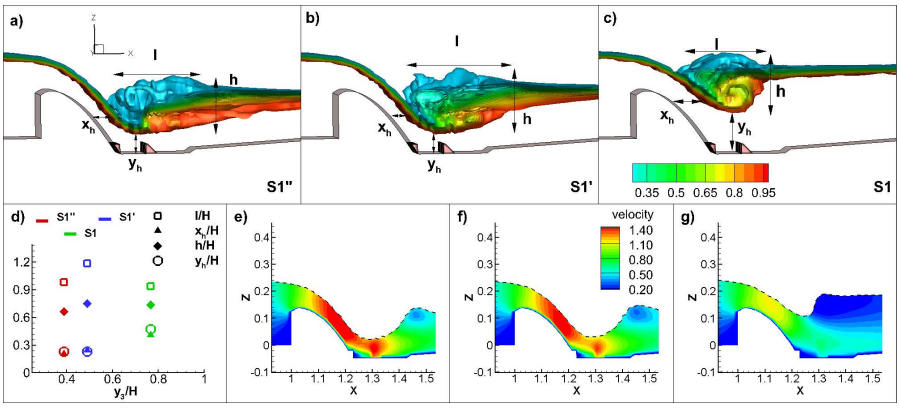

Figure 4: Tail water depth effect in the free surface profile over the spillway and stilling basin; a)Free surface profile for simulation case S1"; b)Free surface profile for simulation case S1'; c)Free surface profile for simulation case S1; d) Adimensional tail water depth versus adimensional jump's length, height and position; e) Velocity profile for simulation case S1"; f) Velocity profile for simulation case S1'; g) Velocity profile for simulation case S1.

4.2 Gate Analysis

In Figure 5 isocontours of VF are shown for the simulation scenarios of the gate and its dissipation basin. It is assumed that 0.35 <VF< 0.95 represents the interface between air and water in simulations. Two flow discharges and three different gate openings were

simulated in three scenarios (G1,G2,G3). Figures 5a,b) illustrate the free surface profile for simulation G1 and G2. Both represent design flow conditions of aproximatetly 400 m^3/s with prototype gate openings of 0.56m and 0.62m, respectively. Additionally, we created simulation G3 to show the free surface profile for an extreme flow condition of 700 m^3/s and a gate opening of 1.32m. Figure 5c) illustrates this simulation. Finally, in Figure 5d) we are showing a picture of the experimental results for flow conditions equivalent to simulation G2. In all figures we indicated the length (l) and height (h) of the hydraulic jump. Good agreement between physical and numerical models is observed qualitatively from Figures 5b,d). The effect of smaller gate opening can be observed by comparing Figures 5a,b). A clear increase of the upstream water depth results for the smallest opening. We determined that a larger gate opening reduces the size of the perturbation produced downstream of the gate.

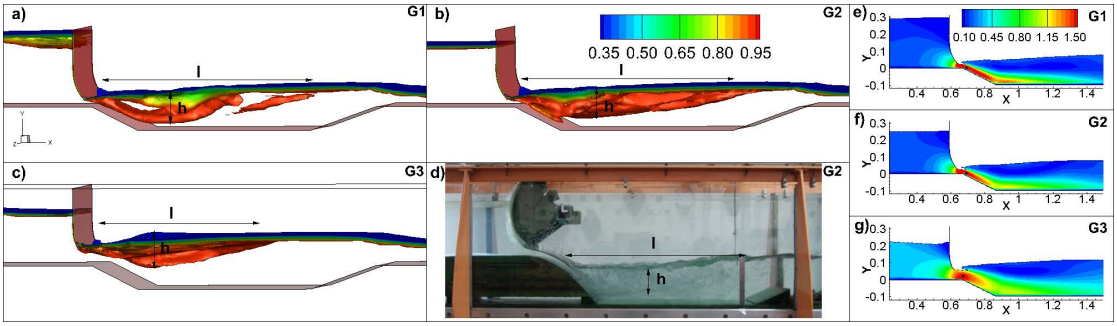

Figure 5: Free surface profile and velocity distribution throughout the simulation domain of the gate and dissipation basin; a)Free surface profile for simulation case G1; b)Free surface profile for simulation case G2; c)Free surface profile for simulation case G3; d) Picture of the physical model for equivalent conditions to G2 simulation; e)Velocity distribution for simulation case G1; f)Velocity distribution for simulation case G2; g)Velocity distribution for simulation case G3. Dot represents the location of maximum velocity.

Figures 5e,g) show velocity distribution for the three simulations scenarios. In these figures the dash line represents the free surface which is defined by VF=0.6. The color band indicates the range of velocity contours shown in the figures. Small gate opening creates high velocities near the bed. The maximum velocity extrapolated to prototype scale was around 11.4m/s. As observed in Figure 5e) the high velocity patch is elongated and enters further into the dissipation basin. As a result, scour at the bottom of the dissipation basin would be expected for this flow condition. Moreover, for design flow condition, we found a 9% velocity reduction under the gate from an 11% increase in the gate opening. Furthermore, we were able to determine that for a flow discharge 1.75 times larger than the design discharge when gate opening is 2.35 times larger than the smallest gate opening the velocity reduction increased to 27%.

Experimental velocity measurements at the middle and end of the dissipation basin were available for the three simulation cases. Table 2 compares the numerical results with the measurements. Reasonable agreement exist between the simulation results and

the physical measurements for G2 and G3 cases. However, for G1 such aggrement is not achieved. Not having information of the tail water depth as downstream boundary condition for the numerical simulations might have caused this variation.

5 CONCLUSIONS

A study of flow interaction with scaled models of an ogee shape spillway and a tainter gate was presented. A fully three-dimensional CFD model was set up for these two hydraulic structures. The numerical model was validated against experimental information. Most of the simulation results are found to be in reasonable agreement with the experimental ones. The outcomes of the simulations, permitted evaluation of the designed structures. Based on the numerical results, the design of the ogee shape spillway and tainter gate were found to be appropriate as the hydraulic jump occurred within the designed basin for all simulation conditions. Furthermore, this study shows that CFD can be used as a design tool of hydraulic structures together with proper experimental analysis for validation. Many more cases could be easily tested with the numerical simulations, which provide detailed information of the flow velocity, vorticity, pressure among other characteristics. Thus, the numerical model showed to have a significant advantage in practice, in terms of parametric studies.

6 Acknowledgements

The writers greatly appreciate the physical model information provided by the research and academic unit PROMAS (Soil and Water Management Program) from the University of Cuenca-Ecuador and by ACSAM Consulting Firm. The support of the Pittsburgh Supercomputing Center (PSC) for providing us with computational time is acknowledged.

REFERENCES

[1] B.M. Savage and M.C. Johnson. *Flow over Ogee Spillway: Physical and Numerical Model Case Study*, Journal of Hydraulic Engineering, August,(2001).

[2] M.C. Johnson and B.M. Savage. *Physical and Numerical Comparison of Flow over Ogee Spillway in the Presence of Tailwater*, Journal of Hydraulic Engineering, 1353–1357,December,(2006).

[3] M.R. Najafi et al. *Numerical Modeling of Flow Condition in a Bottom Outlet*, 16th IAHR-APD Congress and 3rd Symposium of IAHR-ISHS,1817–1822,(2008).

[4] B. Dargahi. *Experimental Study and 3D Numerical Simulations for a Free-Overflow Spillway*, Journal of Hydraulic Engineering,899–907,September,(2006).

[5] C. Turan et al. *Study of the Free Surface Flow on an Ogee-Crested Fish Bypass*, Journal of Hydraulic Engineering,1172–1175,August,(2008).

[6] S. Li et al. *Numerical Modeling of Probable Maximum Flood Flowing through a System of Spillways*, Journal of Hydraulic Engineering,66–74,January,(2011).

[7] D.C. Wilcox. *Turbulence Modeling for CFD*, DCW Industries, Inc. La Canada, California,(1998).

[8] Fluent (ANSYS), 2009, Fluent 12.0 Users Guide.

[9] O. Ubbink and R.I. Issa. *A Method for Capturing Sharp Fluid Interfaces on Arbitrary Meshes*, Journay of Computational Physics,**153**,26–50,July,(1999).

[10] V.T. Chow. *Open-channel Hydraulics*, McGraw-Hill, New York,(1959).

[11] H. Chanson. *Development of the Blanger Equation and Backwater Equation by Jean-Baptiste Blanger (1828)*, Journal of Hydraulic Engineering,ASCE, Vol. 135, No. 3, pp. 159-163,(2009).